Rare Metal Materials and Engineering
Volume 52, Issue 4, April 2023
Available online at www.rmme.ac.cn

Science Press

Cite this article as: An Dongyang, Liu Chenfei, Zhao Shuang, et al. High-Temperature Oxidation Resistance Performance of Si-Ti-Cr Silicide Coating on Nb-Hf Alloy Surface in Constant Oxidation and Thermal Shock[J]. Rare Metal Materials and Engineering, 2023, 52(04): 1219-1226.

ARTICLE

High-Temperature Oxidation Resistance Performance of Si-Ti-Cr Silicide Coating on Nb-Hf Alloy Surface in Constant Oxidation and Thermal Shock

An Dongyang[1,2], Liu Chenfei[1], Zhao Shuang[1], Zhang Haipeng[3], Zou Yongchun[3], Tang Zengwu[1], Xiao Peng[2], Dai Jingmin[2], Wang Yaming[3]

[1] Beijing Xinghang Mechanical-electrical Equipment Co., Ltd, Beijing 100074, China; [2] School of Instrumentation Science and Engineering, Harbin Institute of Technology, Harbin 150001, China; [3] Institute for Advanced Ceramics, Harbin Institute of Technology, Harbin 150001, China

Abstract: To improve the high-temperature oxidation resistance performance of Nb-Hf alloys, Si-Ti-Cr silicide coatings were prepared on Nb-Hf alloy by slurry sintering and high-temperature permeation methods. The high-temperature oxidation resistance performance of Si-Ti-Cr silicide coating on Nb-Hf alloys in high-temperature constant oxidation and high-temperature thermal shock was analyzed, and the failure mechanism of Si-Ti-Cr coating in high-temperature constant oxidation and high-temperature thermal shock was determined. The results show that the mass gain of the coating is 7 mg/cm^2 after constant oxidation at 1800 °C for 5 h. The mass gain of the coating in atmosphere is less than 1.8 mg/cm^2 after thermal shock cycles for 50 cycles followed by constant oxidation at 1700 °C for 5 h. Therefore, the silicide coating exhibits excellent oxidation resistance at 1800 °C in constant oxidation and at 1700 °C in thermal shock/constant oxidation.

Key words: silicide coating; oxidation resistance; thermal shock resistance; constant oxidation; high temperature

Nb-Hf alloy has been widely used in aviation and aerospace owing to its high melting point, high-temperature stable performance, and good mechanical properties under 1000 ℃, which enable it to be used under extreme high-temperature environments at 1200−1400 °C[1–5]. However, the Nb-Hf alloy reacts with fuels in high-temperature oxygenated environment, which seriously affects the mechanical properties and has become a key factor limiting its application[6–7]. Therefore, it is necessary to modify the surface of the Nb-Hf alloy by fabricating high-temperature oxidation resistant coatings[8–10]. As one of the most widely used high-temperature oxidation-resistant coatings, the silicide coating is a functional membrane characterized by thermal insulation, oxidation resistance, corrosion resistance, thermal shock resistance, impact resistance, and prolonged service life[11–13]. It is formed on the surface of the metal or ceramics by the in-situ diffusion of ceramic or metal powder through slurry sintering and high-temperature infiltration. Due to their excellent performance and long working time at high temperatures, silicide coatings can significantly improve the service life of the alloys and expand application fields[14–17]. Silicide coatings are widely used in spacecraft thermal protection systems to protect niobium, hafnium and other matrix materials, wherein the service temperature preferably ranges from 1300 °C to 1800 °C [18–22].

With increasing the requirement for the thrust-weight ratio and reliability of engines, silicide coatings play a critical role in aerospace[23–25]. Research on the oxidation behavior and failure mechanism of silicide coatings is important due to their extremely complex and harsh multi-field coupled high-temperature serve environment[26–28]. Previous work shows that high-temperature oxidation is an important cause of the failure for silicide coatings[29–32]. Qualitative and quantitative analysis of the oxidation resistance of the coatings is carried out by the combination of structure, elements, and quality change. The analysis of the oxidation failure mechanism of silicide

Received date: September 04, 2022
Foundation item: National Defense Technical Basic Research Program of China (JSZL 2015603 B 002); Aviation Science Fund Project (20172777007); National Natural Science Foundation of China (52206225); China Aerospace Science and Industry Corporation Reliability Assurance Project (2021A007)
Corresponding author: An Dongyang, Ph. D., Beijing Xinghang Mechanical-electrical Equipment Co., Ltd, Beijing 100074, P. R. China, E-mail: zdady1989@163.com

coatings can provide effective thinking to improve the oxidation resistance of the coatings.

In this work, the Nb(Cr, Ti)Si_2-Nb_5Si_3 composite gradient silicide coating was prepared on the Nb-Hf alloy by vacuum sintering to explore its high-temperature and thermal-shock oxidation behavior. Furthermore, the three-dimensional heat transfer simulation analysis was used to investigate the mechanism of the heat distribution on the coating surface. Moreover, the qualitative analysis of the microstructure, properties, and protective mechanism of the coating was conducted by the analysis of microstructure and phase composition. Finally, the mass changes of the coatings under different oxidation conditions were characterized by the thermogravimetric method, according to which the high-temperature oxidation resistance of the coatings was evaluated.

1 Experiment

1.1 Coating design

The slurry was sprayed uniformly on the Nb-Hf alloy surface, and then the powder mixture was melted or semi-melted by vacuum melting. Meanwhile, elements of the melt, such as Ti and Si, react with each other or with the matrix and diffuse to form various functional substances in the diffusion transition layer and the dense layer. Finally, the coating was formed by cooling and solidification. The outer layer is composed of complex (Nb, Cr, Ti)Si_2 phases. The diffusion transition layer is composed of dense mixed phases with the coexistence of the (Nb,Ti)Si_2 and (Nb,Ti)$_5Si_3$ phases. When the coating is exposed to the high temperature above 1300 °C in the air, the constituent elements in the coating will undergo an oxidation reaction to form (Nb,Cr,Ti,Si)$_xO_y$, which prevents the diffusion of oxygen to the coating-substrate interface and improves the oxidation resistance of the alloy.

1.2 Sample preparation

The Nb-Hf alloy (NbHf 10-1) with a size of 70 mm×10 mm×1 mm was selected as the sample sheet. The surfaces were polished with sandpaper, then cleaned with acetone, and dried for later use. The slurry was prepared by selecting the proper proportion of powders with Si, Cr, and Ti as the main components in the system. Some functional elements such as binders and diluents were added, and the slurry was evenly sprayed onto the surface of the sample sheet. At last, the sample sheet was kept in a vacuum sintering furnace at 1400–1500 °C for 10 – 30 min to fabricate the coating with a thickness of 0.1 mm.

1.3 Characterization techniques

(1) A scanning electron microscope (SEM, Quanta 200 FEG, USA) with an operating voltage of 20 kV was used for investigating the surface and cross-sectional morphologies of the coatings. X-ray diffraction (XRD, Empyrean, Panalytical, Netherlands) with a Cu Kα radiation working at 30 mA and 40 kV was used for characterizing the phase compositions.

(2) Characterization of the high-temperature oxidation resistance. The oxidation resistant performance test at 1300, 1400, 1700 and 1800 °C for 5 h of the coated specimens (70 mm×10 mm×1 mm) was carried out by the high-temperature thermal shock test-bed. Then the heating device was turned off to analyze the oxidation behavior of the coating.

(3) Characterization of the air-cooled thermal shock resistance. Through a high-temperature thermal shock test rig, the coated sample sheet (70 mm×10 mm×1 mm) was heated to 1500 and 1700 °C for 15 s and kept for 10 s, and then immediately cooled to 500 °C by air cooling. Thus, one thermal shock cycle was finished and the thermal shock life was recorded. The test device is shown in Fig.1.

Fig. 2a is a three-dimensional heat transfer model of the niobium-hafnium alloy with silicide coating. Both edges of the sample are clamped by brass electrodes with good conductivity and heated to the experimental temperature by electrification. The temperature is controlled by an infrared optical fiber temperature sensor. Fig.2b is a three-dimensional temperature field simulation of the sample in the process of induction heating. The middle part of the sample shows the highest temperature and radiates the most energy outward. Therefore, it can be speculated that the coating is damaged in the middle part first and then the damage spreads to both edges. According to this, the microstructural changes of the middle part of the coating before and after the experiment are mainly analyzed for the characterization of oxidation resistance and thermal shock resistance of the coating.

2 Results and Discussion

The microstructures of the coatings after oxidization in the air at 1300, 1400, 1700 and 1800 °C for 6 h were compa-

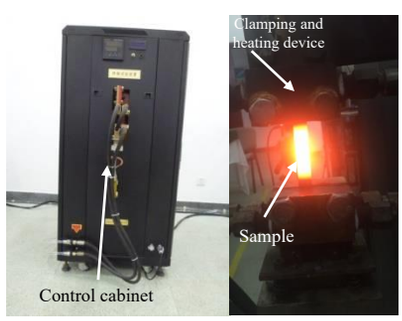

Fig.1 Air thermal shock and oxidation performance test device

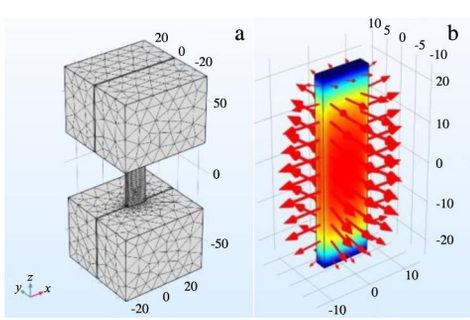

Fig.2 Physical model of grid structure (a) and three-dimensional temperature field simulation (b) of coated specimen

ratively investigated to evaluate the high-temperature oxidation resistance of the coatings. Besides, the thermal shock resistance of the coatings in the air at 1500 and 1700 °C was also studied to evaluate the thermal shock resistant performance of the coatings in air. Furthermore, the thermal shock failure mechanism of the coatings was explained by microstructural changes.

2.1 XRD analysis

The phase composition of the coatings oxidized in air at 1300, 1400, 1700 and 1800 °C for 6 h is shown in Fig. 3. The main phases of the coatings are $NbSi_2$ and Nb_5Si, and a small amount of $CrSi_2$ is found, which is consistent with the phase of the matrix coating. A small number of oxides, such as SiO_2, Cr_2O_3 and Nb_2O_5, appear in the coatings after oxidation at the medium temperature of 1300 and 1400 °C for 6 h, which indicates that the coatings begin to be oxidized. When the temperature rises to 1700 and 1800 °C, the content of SiO_2 in the coatings increases obviously ($4NbSi_2+13O_2=8SiO_2+2Nb_2O_5$), which indicates that the high temperature promotes the further oxidation of the element Si and accelerates the transformation from silicide coating to oxide coating.

Fig. 4a shows the XRD patterns of the coatings after 150 cycles of thermal shock cycles in the air at 1500 °C. The main phases of the coatings after the thermal shock are $NbSi_2$, Nb_5Si_3, SiO_2, and a small amount of NbO_2 and Nb_2O_5, which indicates that the oxidation mechanism of the coatings during the thermal shock is consistent with that of the isothermal oxidation. The XRD patterns of the coatings after thermal shock at 1700 °C for 50 cycles followed by continuous oxidization at the same temperature for 5 h are shown in Fig. 4b. The phase compositions of the coatings after the thermal shock are consistent with that after oxidization for a certain time, which further indicates that the coatings have the

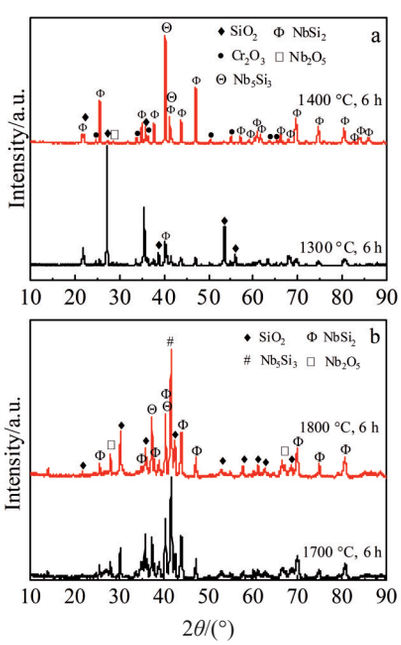

Fig.3 XRD patterns of the coating oxidized at medium temperature (a) and high temperature (b) for 6 h

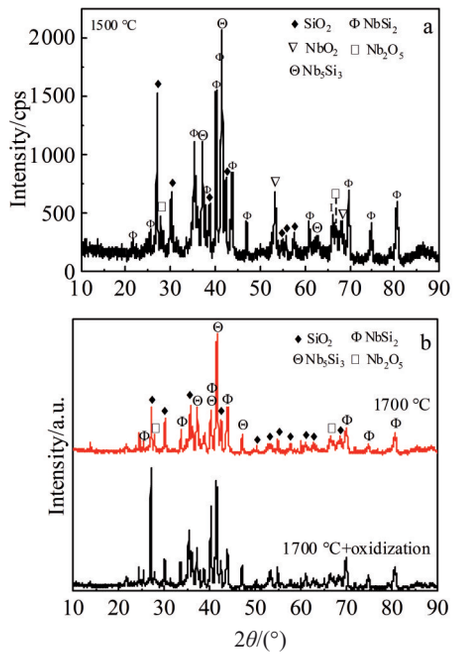

Fig.4 XRD patterns of coatings after thermal shock cycles at 1500 °C for 150 cycles (a) and 1700 °C for 50 cycles followed by continuous oxidization for 5 h (b)

same reaction and mechanism in the thermal shock and isothermal oxidation.

2.2 Microstructure and elemental composition

Fig. 5 is the microstructure of the silicide coating on the surface of the Nb-Hf alloy (NbHf 10-1). It can be seen from the surface morphology in Fig. 5a and 5b that the rod-shaped grains are sintered. Also, there are many pores on the surface, which will increase the area of oxidation. However, from the cross-section morphology in Fig. 5c, it can be observed that the pores only exist in the outer layer but the inner part of the coating is still densely bonded. Through the analysis of the sintering process, it is believed that they are caused by the volatilization of the additives during the surface sintering. Moreover, according to the cross-section morphology, it can be seen that the silicide coating is a double-layer composite structure with a transition layer (Nb_5Si_3 layer) between the substrate and the outer layer ($NbSi_2$ layer). The cross-section morphology also shows that the total thickness of the coating is about 97.2 and 8.6 μm for the transition layer, and 88.6 μm for the outer layer. Fig. 6 shows the EDS spectra at different locations of the cross-section of the composite coating. From EDS results, it can be concluded that the element ratio of the transition layer is Si:Nb=0.59, indicating that the Nb_5Si_3 phase is formed by diffusion. While the element ratio of the outer layer is Si:Nb=1.9, indicating that the $NbSi_2$ phase is formed by diffusion.

The composite coating contains the transition layer, and the substrate can be protected well by the transition layer which will further inhibit the diffusion of oxygen after the complete oxidization of the outer layer ($NbSi_2$ layer). Therefore, the oxidation resistance of the composite coating is better than

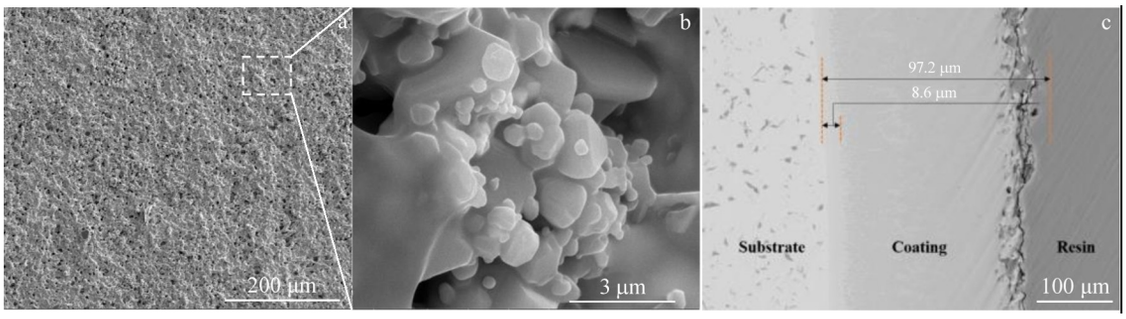

Fig.5 SEM morphologies of surface (a, b) and cross-section (c) of original coating

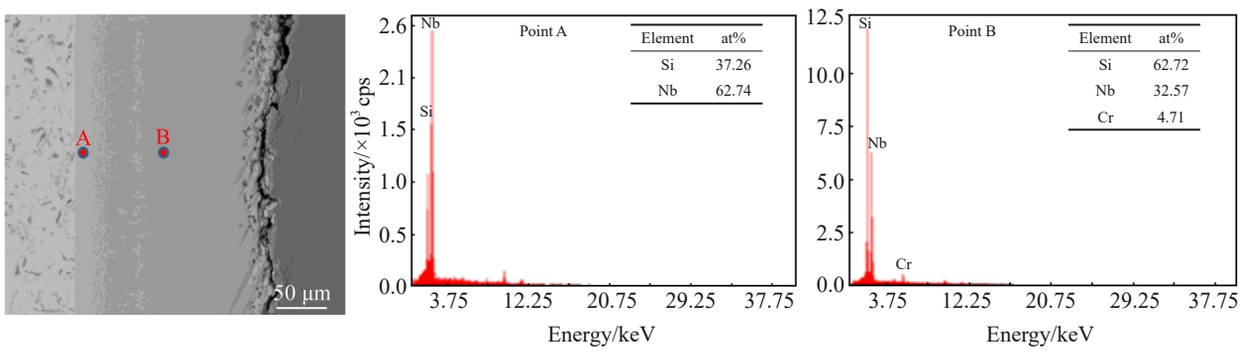

Fig.6 SEM image and EDS results of the original coating

that of the single silicide coating. Fig. 7 presents the micro-morphology of the coatings after 6 h oxidation at the medium temperature of 1300 and 1400 °C and at the high temperature of 1700 and 1800 °C. It can be seen that the pores on the surface are fewer than on the silicide coating. Fewer pores reduce the oxidation area. After isothermal oxidation at 1300 and 1400 °C, the surface of the coating is loose with a few microcracks. This is mainly due to the mismatch of the thermal expansion coefficient between the coating and the matrix at high temperature, which produces thermal stress inside the coating and some cracks. From the high magnification, it can be seen that the grains existing independently are observed, which are similar to the mastoid. However, the surface of the coating after isothermal oxidation at 1700 and 1800 °C is denser than that at 1300 and 1400 °C, and the cracks disappear. At high magnification, the bonding between grains is observed, and the bonding material is similar to the binder. When the isothermal oxidation happens at 1700 and 1800 °C, it can be seen in Fig. 3 that a large amount of SiO_2 is generated on the coating surface. Since it is molten at a high temperature (1650 °C), silica can act as a high-temperature binder to connect grains, forming a dense coating to prevent the diffusion of oxygen, thus improving the oxidation resistance of the coating. Therefore, SiO_2 plays an important role as high-temperature coating material.

Through the analysis of the microstructure in the middle-temperature state, it can be inferred that the coating after isothermal oxidation at 1700 and 1800 °C should have cracks, but they are repaired by the glass-like SiO_2. Consequently, the occurrence of cracks can only be observed through the cross-section morphology. As shown in Fig. 8, there are few internal cracks after the isothermal oxidation at the medium temperature of 1300 and 1400 °C, the cracks occur on the surface of the coating. However, after the isothermal oxidation at 1700 and 1800 °C, the surface cracks are healed by the glass-like SiO_2 so that the oxygen cannot diffuse into the coating. But, the glass-like SiO_2 does not form inside the coating to heal the cracks, which can be observed from the cross-section morphology.

The surface and cross-section morphologies of the coatings after the thermal shock cycle in the air are shown in Fig. 9 and Fig. 10. After 150 cycles of thermal shock at 1500 °C, the surface of the coating is covered with microcracks. However, from the cross-section morphology, it can be seen that some cracks penetrate the interface of the coating and substrate, which greatly reduces the oxidation resistance of the coating. When the temperature rises to 1700 °C, the microcracks disappear on the coating surface. But, there are still penetrating cracks and even a large number of holes in the cross-section. The reason is that when the temperature rises to 1700 °C, the oxygen partial pressure increases to form gaseous SiO. The volatilization of the SiO further results in the formation of pores inside the coating. These pores are then repaired by liquid SiO_2. Under the condition of thermal shock quenching, SiO_2 is solidified into a glaze state, thus repairing surface microcracks, but there are still large penetrating cracks and pores in the coating.

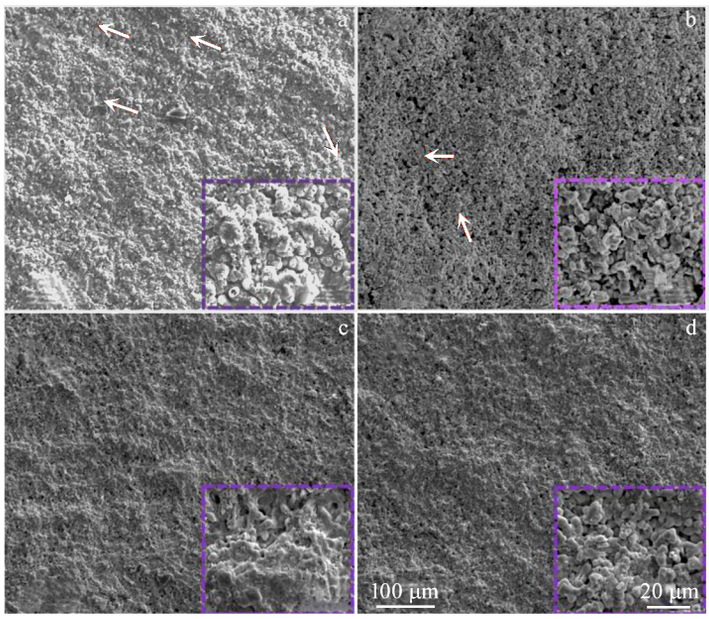

Fig.7 Micro-morphologies of coatings held at different temperatures for 6 h: (a) 1300 °C, (b) 1400 °C, (c) 1700 °C, and (d) 1800 °C

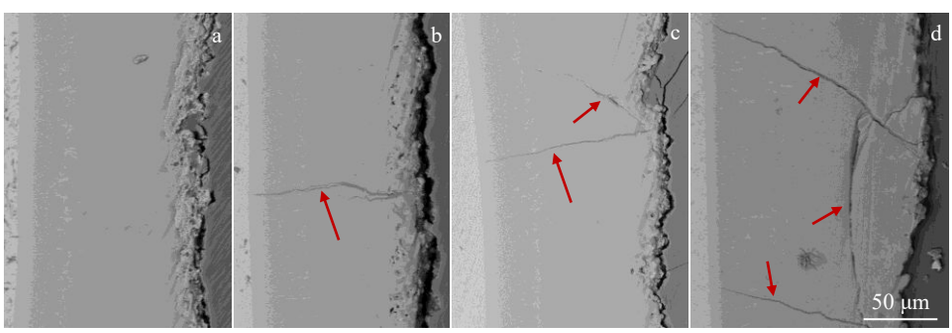

Fig.8 Cross-section morphologies of coatings held at different temperatures for 6 h: (a) 1300 °C, (b) 1400 °C, (c) 1700 °C, and (d) 1800 °C

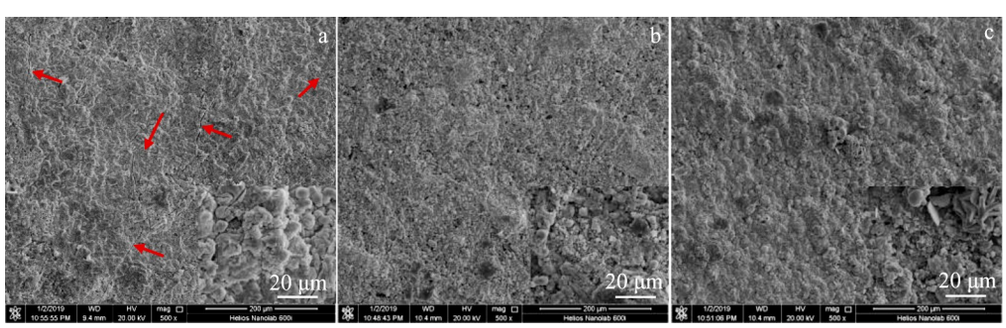

Fig.9 Micro-morphologies of coating after 150 cycles of thermal shock at 1500 °C (a) and 50 cycles of thermal shock at 1700 °C (b) followed by oxidization for 5 h (c)

2.3 Mass variation

As shown in Fig. 11, the coating mass increases gradually after isothermal oxidization in the air, because the oxygen in the air continuously diffuses into the coating at high temperatures. The higher the oxidation temperature, the easier it is for the oxygen to diffuse into the coating, and the greater the coating mass gain within the same period. From the morphology analysis, it is found that no penetrating cracks appear in the coating after the isothermal oxidization at 1300 and 1400 °C, which make it tough for the oxygen to diffuse into the coating. However, the cracks penetrate through the interface of the membrane and the substrate due to isothermal oxidization at 1700 and 1800 ° C, which induces more diffusion paths for the oxygen available, thus causing larger

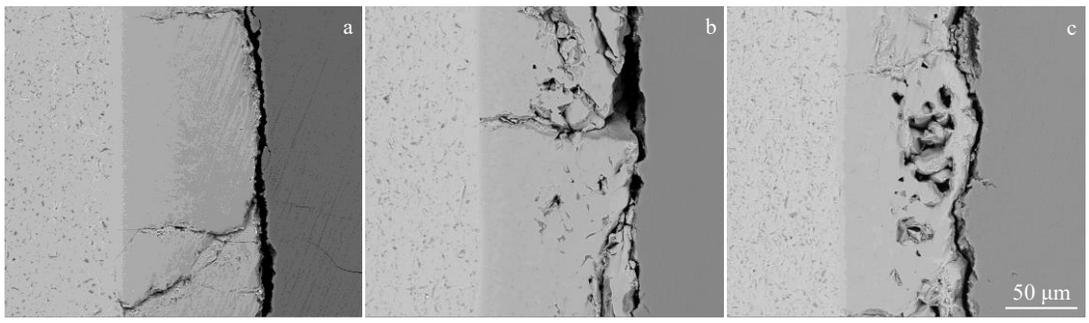

Fig.10 Cross-section morphologies of coating after 150 cycles of thermal shock at 1500 °C (a) and 50 cycles of thermal shock at 1700 °C (b) followed by continuous oxidization for 5 h (c)

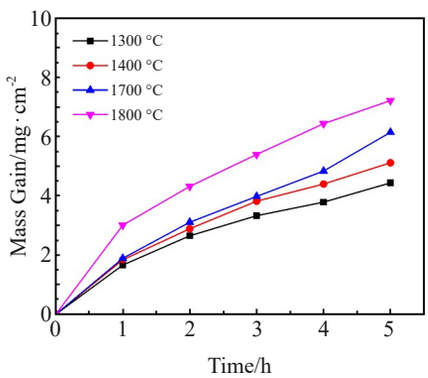

Fig.11 Oxidation kinetics curves during isothermal oxidization of the coatings at different temperatures for 5 h

mass gain of coating. At 1800 °C, the mass gain of the coating is rapid with a maximum value of 7 mg/cm^2. At this time, the coating might have failed and lost its protective effect on the substrate.

As shown in Fig. 12a, the coating mass gain increases continuously during the 150 cycles of thermal shock in the air at 1500 °C. In the first 10 cycles of thermal shock tests, the mass gain of the coating is the fastest, totally increased by 1.2 mg/cm^2. Then it increases slowly to 2.6 mg/cm^2. The coating also shows the same trend in the thermal shock cycle test at 1700 °C. The mass gain of the coating is 1.3 mg/cm^2 in the first 10 cycles, and then it increases slowly to 1.9 mg/cm^2. When the sample is isothermally oxidized for 5 h after thermal shock at 1700 °C, the coating mass is increased by about 1.8 mg/cm^2. This indicates that the oxidation mass gain of the coating is in the initial stage of the thermal shock test, at which the oxygen in the air reacts rapidly with the (Nb, Cr, Ti) Si_2 in the surface layer to form corresponding oxides. Then at high temperatures, the oxygen continues to diffuse through the defects to the interior. After 10 cycles of thermal shock at 1700 °C, the mass gain of the coating slows down. The reason can be inferred from the surface and interface morphologies. The liquid SiO_2 formed at 1700 °C will become a layer of glass-ceramic film on the surface of the coating under air-cooling conditions to prevent inward oxygen diffusion.

2.4 Heat distribution simulation

Fig.13 shows the surface temperature rising curve and three-dimensional temperature distribution of the Nb-Hf alloy (NbHf 10-1 alloy) with 0.1 mm coating heated to 1500 °C by direct electric heating. The temperature of the sample sheet rises rapidly to 1500 °C within 30 s, and gradually decreases from the middle part to both edges. The maximum temperature in the middle is 1502 °C. Temperature gradient distribution induces thermal stress in the coating. The largest thermal stress is in the middle part of the sample where the coating failure occurs first, and typically failure morphology

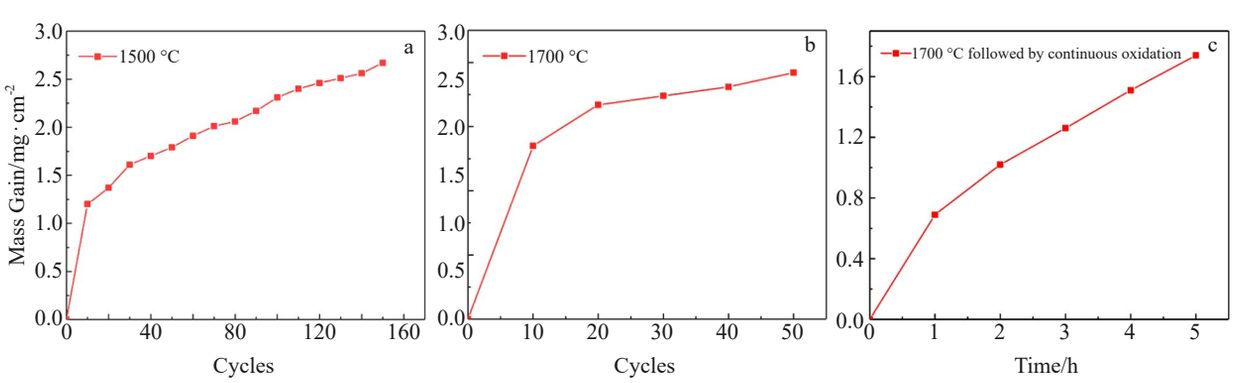

Fig.12 Mass gain curves of coating after 150 cycles of thermal shockat 1500 °C (a) and 50 cycles of thermal shock 1700 °C (b) followed by continuous oxidization for 5 h (c)

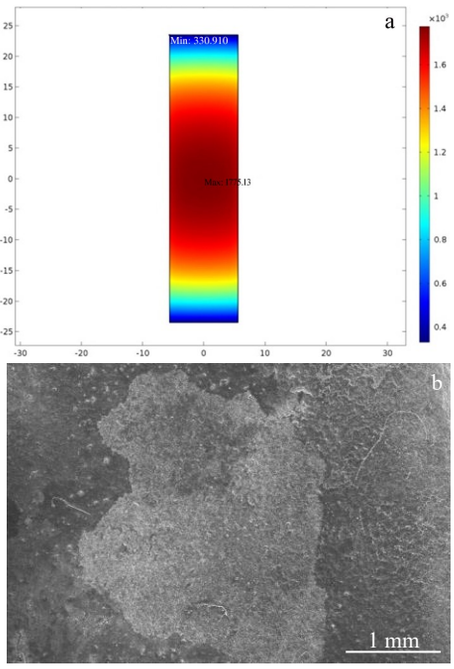

Fig.13 Surface temperature distribution at 1500 °C (a) and micromorphology of failure coating (b)

is presented in Fig.13b.

3 Conclusions

1) The composite silicide coating with 0.1 mm in thickness is prepared by slurry sintering and high-temperature infiltration. The interface transition layer is the Nb_5Si_3 phase and the outer layer is the $NbSi_2$ phase formed through the diffusion of silicon and alloy elements. The coating is dense and well-bonded with the substrate.

2) The coating's mass gain increases with the oxidation time and temperature from 1300 °C to 1800 °C when the coatings are oxidized isothermally. SiO_2 is generated when the silicide coating is oxidized isothermally above 1200 °C, and melted above 1650 °C to repair the coating surface cracks and to increase oxidative resistance.

3) According to the simulation of the heat distribution of a sample with 0.1 mm thick coating, the sample in the experiment device will lose efficacy from the middle part first. The thermodynamic and dynamic processes of silicon and oxygen play a decisive role in the oxidation resistance of silicide coatings during isothermal oxidation and thermal shock. To further improve the comprehensive performance of the coatings, the thickness, composition, and structure of the coatings can be optimized firstly to prepare multi-gradient composite coatings.

References

1 Da S L, Claro A P, Donato T A. *Artificial Organs*[J], 2011, 35(5): 516

2 Lepienski C M, Meruvia M S, Veiga W. *International Journal of Materials Research*[J], 2011, 95 (10): 1405

3 Du S, Zhang C, Bian L *et al*. *Rare Metal Materials and Engineering*[J], 2018, 47(11): 3548

4 Ren H, Liu F, Lin X *et al*. *Rare Metal Materials and Engineering*[J], 2019, 48(10): 3289

5 Zhang C, He X, Lan X *et al*. *Rare Metal Materials and Engineering*[J], 2010, 39(12): 2232 (in Chinese)

6 Ge Y L, Wang Y M, Chen J C, *et al*. *Journal of Alloys and Compounds*[J], 2018, 745: 271

7 Xie S M, Lin S S, Shi Q *et al*. *Surface and Coatings Technology*[J], 2021, 413: 127 092

8 Kumar S and Kumar R. *Surface Engineering*[J], 2021, 37(11): 1339

9 Cui Y, Shen J Q, Manladan S M *et al*. *Applied Surface Science*[J], 2020, 512: 145 736

10 Gu X N. *Acta Biomater*[J], 2011,7(4): 1880

11 Wang W, Zhou C. *Corrosion Science*[J], 2016, 110: 114

12 Fu Q G, Li H J, Shi X H *et al*. *Surface and Coatings Technology*[J], 2006, 201(6): 3082

13 Xu H, Wang H, Liu J H *et al*. *Corrosion Science*[J], 2020, 173: 108 752

14 Knittel S, Mathieu S, Portebois L *et al*. *Surface and Coatings Technology*[J], 2013, 235: 401

15 Chakraborty S P, Banerjee S, Sharma I G. *Journal of Nuclear Materials*[J], 2010, 403 (1–3): 152

16 Mitra R. *International Materials Reviews*[J], 2006, 51 (1): 13

17 Tang Z H, Thom A J, Kramer M J. *Intermetallics*[J], 2008,16(9): 1125

18 Vilasi M, Francois M, Podor *et al*. *Journal of Alloys and Compounds*[J], 1998, 264: 244

19 Bewlay B P, Jackson M R, Zhao J C *et al*. *Metallurgical and Materials Transactions A-Physical Metallurgy and Materials Science*[J], 2003, 34: 2043

20 Cockeram B V. *Surface and Coatings Technology*[J], 1995, 76: 20

21 Perepezko J H. *Science*[J], 2009, 32(6): 1068

22 Ge Y L, Wang Y M, Chen J C H *et al*. *Journal of Alloys and Compounds*[J], 2018, 767: 7

23 Ho C H, Prakash S, Deshpandey C V *et al*. *Surface and Coatings Technology*[J], 1989, 39 (1–3): 79

24 Yan Z, Feng C, Xiang X J. *Journal of Composite Materials*[J], 2010, 44 (26): 3085

25 Du J, Du P Y, Xu M *et al*. *Journal of Non-crystalline Solids*[J], 2008, 354 (12–13): 1308

26 Wang W, Zhang B Y, Zhou C G. *Corrosion Science*[J], 2014, 86: 304

27 Sun J, Fu Q G, Guo L P *et al*. *ACS Applied Materials and Interfaces*[J], 2016, 8 (24): 15 838

28 Chakraborty S P, Banerjee S, Sharma I G *et al*. *Journal of Nuclear Materials*[J], 2010, 403 (1–3): 152

29 Wang C, Wang W, Zhu S L *et al*. *Corrosion Science*[J], 2013,

76: 284

30 Kong M, Zhao W J, Wu Y *et al*. *Journal of Coatings Technology and Research*[J], 2012, 9 (2): 177

31 Inturi S N R, Boningari T, Suidan M *et al*. *Industrial and Engineering Chemistry Research*[J], 2016, 55(46): 11 839

32 Thomas K S, Varma S K. *Corrosion Science*[J], 2015, 99: 145

Nb-Hf 合金表面 Si-Ti-Cr 硅化物涂层在恒温氧化和热震中的高温抗氧化性能

安东阳[1,2]，刘晨飞[1]，赵　爽[1]，张海鹏[3]，邹永纯[3]，唐增武[1]，萧　鹏[2]，戴景民[2]，王亚明[3]

(1. 北京星航机电装备有限公司，北京 100074)

(2. 哈尔滨工业大学 仪器科学与工程学院，黑龙江 哈尔滨 150001)

(3. 哈尔滨工业大学 特种陶瓷研究所，黑龙江 哈尔滨 150001)

摘　要：为了提高Nb-Hf 合金的高温抗氧化性能，采用浆料烧结和高温渗透制备了Si-Ti-Cr硅化物涂层。分析了Si-Ti-Cr 硅化物包覆的Nb-Hf 合金样品在恒温氧化和高温热震条件下的抗氧化性能，揭示了Si-Ti-Cr 涂层高温恒温氧化和高温热震条件下的失效机理。结果表明，在1800 ℃恒温氧化5 h条件下，涂层的增重为7 mg/cm^2；在1700 ℃热震循环50周次和恒温氧化5 h条件下，涂层的最大增重为1.8 mg/cm^2。硅化物涂层在1800 ℃恒温氧化环境下和1700 ℃热震/恒温氧化环境下具有优异的抗氧化性能。

关键词：硅化物涂层；抗氧化；热震性能；恒温氧化；高温

作者简介：安东阳，男，1989年生，博士，北京星航机电装备有限公司，北京 100074，E-mail：zdady1989@163.com